UCLA
UCLA Previously Published Works

Title
Steady-state directional diffuse reflectance and fluorescence of human skin

Permalink
https://escholarship.org/uc/item/0m85r4xf

Journal
Applied Optics, 45(17)

ISSN
0003-6935

Authors
Katika, K M
Pilon, L

Publication Date
2006-06-01

Peer reviewed

eScholarship.org Powered by the California Digital Library
University of California

Steady-State Directional Diffuse Reflectance and Fluorescence of Human Skin

Kamal M. Katika and Laurent Pilon

Mechanical and Aerospace Engineering Department

Henri Samueli School of Engineering and Applied Science

University of California, Los Angeles - Los Angeles, CA 90095, USA

Phone: +1 (310)-206-5598, Fax: +1 (310)-206-2302

pilon@seas.ucla.edu

This paper presents numerical simulations predicting the directional diffuse reflectance and autofluorescence from human skin. Skin is modeled as a seven-layered medium with each layer having its own optical properties and fluorophore concentrations. Both collimated and diffuse monochromatic excitation at 442 nm are considered. In addition, the effect of an index matching cream used to eliminate total internal reflection within the skin is assessed. The intensity distributions of the excitation and fluorescence light in the skin are computed by solving the radiative transfer equation using the modified method of characteristics. It was found that the use of an index matching cream reduces the directional fluorescence signal while increasing the directional diffuse reflectance from the skin for collimated excitation. On the other hand, both the fluorescence and diffuse reflectance increase for diffuse excitation with an index matching cream. Moreover, the directional fluorescence intensity obtained using collimated excitation is larger than that was obtained using diffuse excitation light. This computational tool could be valuable in designing optical devices for biomedical applications. © 2006 Optical Society of America

OCIS codes: 170.3660, 170.7050, 290.7050, 300.2530

1. Introduction

Fluorescence is the physical phenomenon in which light is emitted by a substance as a result of excited electrons returning to their ground states after absorption of excitation light. Substances that emit fluorescence (fluorophores) are characterized by their quantum yield, their fluorescence lifetime(s), and their emission wavelengths. Emission takes place over a spectral range and at wavelengths longer than the excitation wavelength. The quantum yield is the ratio of the number of photons emitted to the number absorbed while the fluorescence lifetime is the average time the electrons spend in their excited states.[1]

Biological tissues contain several endogenous fluorophores such as NADH, aromatic amino acids like tryptophan and structural proteins such as collagen and elastin.[2] The optical properties of these fluorophores are sensitive to the environment and the metabolic status of the tissue making fluorescence spectroscopy a valuable tool to study the health of biological tissues.

Practically, fluorescence spectroscopy techniques consist of exposing the medium or tissue of interest to excitation light (typically UV) and measuring the fluorescence emission spectrum. The incident excitation can be a continuous or an ultra-short pulse beam of light. It can also be collimated or diffuse whether a laser or a diffuse light source is used. These measurements can be carried out in (i) a monochromatic or spectral and (ii) steady-state or time-resolved manner. Spectral measurements typically

involve either emission spectra measurements or excitation spectra measurements. Fluorescence emission spectrum measurements consist of measuring the fluorescence intensity over a range of wavelengths for a fixed excitation wavelength. On the contrary, excitation spectra measurements consist of measuring the fluorescence intensity at a particular wavelength for a range of excitation wavelengths.

On the other hand, time-resolved measurements involve measuring the lifetime of the fluorophores. To do so, the sample of interest is exposed to a pulse of light and the intensity decay is recorded using a high-speed detection system. The advantage of time-resolved over steady-state measurements is that they provide more information on the shape, flexibility and conformation state of the fluorescing molecules.[1] This enables identification of different conformations of a molecule which would not otherwise be possible using steady-state measurements. However, time-resolved meaurements require complex and expensive instrumentation unlike steady-state measurements.[1]

In both steady-state and time-resolved fluorescence, the fluorophores are present throughout the tissue and the fluorescent light is absorbed and scattered before emerging from the tissue and reaching the detector. Thus, measurements of the fluorescent light leaving the tissue strongly depend on its optical properties. In order to capture the effects of the tissue's optical properties on the fluorescence signal and those of other parameters such as the geometry of the optical setup, an accurate model of excitation and fluorescent light transport in tissue is needed.

This paper focuses on simulating steady-state excitation and fluorescence light

transport in human skin. The spatial and directional intensity distributions of excitation and fluorescent light within the skin are computed by solving the radiative transfer equation using the modified method of characteristics.[3] The numerical results are then used to predict the steady-state directional diffuse reflected and fluorescence intensity of human skin.

2. Current State of Knowledge

Steady-state fluorescence spectroscopy measurements have been used as a means of diagnosing a variety of diseases. The reader is referred to Refs. 2 and 4 for exhaustive discussions of biomedical applications of steady-state fluorescence measurements. This section reviews studies focusing on autofluorescence of human skin for diagnosing diseases affecting its biochemistry.

Skin is a multi-layered structure with irregular interfaces and layers having anisotropic optical properties.[5] There are several chromophores in the skin which absorb light. The most dominant chromophores are melanin and hemoglobin both of which absorb light in the UV (330-400 nm) and the visible (400-700 nm) part of the spectrum. In general, absorption by proteins becomes dominant at shorter wavelengths (280-330 nm).[6] Some chromophores present in the skin also fluoresce when exposed to UV light including porphyrins, NAD/NADH, tryptophan, collagen cross links, elastin crosslinks, and keratin.[6] These fluorophores are distributed in different layers of the skin and contribute to the overall autofluorescence of the skin.

Steady-state autofluorescence of skin has been considered for in-vivo detection of various skin diseases and pathologies such as acne,[7] aging,[8–10] photoaging due to prolonged exposure to sunlight,[11] psoriasis,[12] skin cancer,[4,13–17] and diabetes.[18] Table 1 summarizes these studies and the emission and excitation wavelengths used. In addition, numerous studies have been performed on the influence of pigmentation[19–21] and photobleaching[22] on the autofluorescence spectrum of human skin.

König *et al.*[7] performed in-vivo steady-state fluorescence spectroscopy measurements on patients with and without acne vulgaris. The authors used a Krypton laser with excitation at 407 nm and were able to identify spots containing bacteria responsible for acne. They concluded that autofluorescence measurements can be used to diagnose acne.

In addition, Na *et al.*[10] studied in-vivo steady-state fluorescence emission intensity at 375 nm from skin at the buttock after being excited by UV light at 330 nm and found that the emission increases with age. They showed that fluorescence emission from skin at this excitation wavelength can be used as a marker for skin aging. Similarly, Sandby-Moller *et al.*[11] found that the fluorescence emission at 455 nm from skin locations other than the buttock after being excited by light at 370 nm strongly correlated with age.

Moreover, Gillies *et al.*[12] used both in-vivo and ex-vivo fluorescence excitation spectra measurements to study psoriasis. First, they identified various excitation bands in human skin corresponding to different fluorophores in different layers of the skin:

(i) tyrosine is mainly confined to the epidermis, (ii) tryptophan is present in the dermis and epidermis, and (iii) collagen and elastin are confined to the dermis. The authors then, compared excitation spectra from psoraitic and normal skin and found an increased absorption due to tryptophan in psoriatic skin. This was consistently observed in psoriatic patients. They thus, concluded that fluorescence spectrocopy is a promising technique for the investigation of psoriasis.

Steady-state fluorescence spectroscopy has also been used to study skin cancer. Brancaleon *et al.*[13] studied in-vivo and ex-vivo skin steady-state autofluorescence excitation and emission spectra and observed that both in basal cell carcinomas (BCC) and squamous cell carcinomas (SCC), the endogeneous fluorescence attributed to tryptophan residues was more intense in tumors than in normal skin. Their results showed that endogeneous fluorescence of non-melanoma skin cancers, excited in the UV region of the spectrum has characteristic features that are different from normal skin and may be exploited for non-invasive diagnostics and for the detection of tumor margins.[13] Moreover, Zeng *et al.*[4,14,15,22–27] combined numerical and experimental tools to study spectral autofluorescence emission from skin and its applications to skin cancer. Zeng and coworkers[28] experimentally studied the steady-state autofluorescence from biopsied skin samples. The authors also numerically simulated the transport of excitation and fluorescent light at various wavelengths using the Monte Carlo method combined with a seven layer optical model of human skin.[23,27] Good agreement was found between experimentally observed fluorescence from human skin

samples and numerical simulations. They further used their experimental technique to diagnose skin cancer.[4,14,15] Zeng and MacAulay[4] then, performed in-vivo clinical trials to test the viability of fluorescence spectroscopy as a diagnostic tool for skin cancer. They were able to distinguish basal cell carcinomas or BCCs from non-cancerous lesions with a sensitivity of better than 85 % and a specificity of about 75 %. Similar studies by Panjehpour[16] and Vo-Dinh[17] also showed that laser-induced fluorescence spectroscopy at an excitation wavelength of 410 nm could be used as an in vivo technique for detection of squamous cell carcinoma, basal cell carcinoma, and pre-cancerous lesions.

More recently, steady-state fluorescence spectroscopy has also been used in the study of diabetes. Indeed, Meerwaldt *et al.*[18] performed in-vivo steady-state autofluorescence emission measurements of the skin on the forearm of patients suffering from type 1 and type 2 diabetes. They excited the skin using a UV lamp with a peak emission at 350 nm and measured the emission intensity from 300 to 600 nm. The authors showed that non-invasive measurements of autofluorescence from skin could be a tool to assess the risks of complications due to accumulation of Advanced Glycation End products (AGEs) in patients suffering from diabetes mellitus.

Moreover, numerical simulations of steady-state autofluorescence from skin have been performed. One of the most common numerical tools used to study reflectance and fluorescence in biological tissue is the Monte Carlo method.[23,29–31] It is a statistical method consisting of tracing the history of a statistically meaningful number of

photons from their points of emission to their points of absorption.[32] The main advantage of the Monte Carlo method resides in its simplicity and ability to deal with complex problems with relative ease. On the other hand, since it is a statistical method it is prone to statistical errors.[32] Churmakov *et al.*[33] studied the steady-state spatial distribution of fluorescence in skin using a two-dimensional Monte Carlo method. Their numerical model takes into account the spatial distribution of fluorophores in skin, and in particular the packing of the collagen fibers. It was used to simulate fluorescence from a layer of fluorescent polymeric nanoparticles transferred onto the skin like a tattoo. These devices could be used for health monitoring or evaluation of cosmetics.[34] They also numerically studied the effect of matching the refractive index at the skin surface with the surrounding medium and concluded that it improves the spatial localization of the fluorescence signal from the skin.[34–36] Furthermore, the diffusion approximation of the radiative transfer equation has also been used extensively to study light transport in biological tissue.[37,38] However, Hielscher *et al.*[39] have shown that the diffusion approximation fails to predict the fluence accurately for tissues with very low scattering and absorption coefficients. The diffusion approximation also gives inaccurate results in highly absorbing tissue.[39] Also, it is difficult to describe collimated sources using the diffusion approximation without carefully choosing the source terms.[40]

Moreover, Yoon *et al.*[41] compared the diffusion approximation with the solution of the radiative transfer equation using the discrete ordinates method for a 1-D absorb-

ing and scattering slab illuminated by a collimated beam of light. Various quantities such as the diffuse intensity (or radiance), total fluence, and diffuse flux were computed. The effect of the optical transport coefficients such as the single scattering albedo (from 0 to 1) and the scattering anisotropy factor on the accuracy was also studied. The authors concluded that the diffusion approximation does not yield accurate angular profiles of the intensity except at locations far from the source and the boundaries.[41] Furthermore, they showed that the diffusion approximation estimates low reflection and high transmission for forward scattering and is not recommended for a highly anisotropically scattering medium.[41] The Monte Carlo method on the other hand, can be used to compute the directional reflected and fluorescence intensities.[42] However, such calculations would be extremely computationally intensive in terms of CPU time and storage capacity in order to obtain statistically meaningful results.

To the best of our knowledge, no study has numerically or experimentally explored the directional variation of the fluorescence emission from human skin. However, the angular profile of the reflectance and the fluorescence signals, could be valuable in designing optical devices for biomedical applications. In addition, biological or morphological changes of the human skin caused by aging or diseases could also affect the directional reflectance and fluorescence signals by changing the scattering phase function and refractive index of the skin layers. Thus, this paper presents numerical simulations of the directional reflectance and fluorescence of human skin exposed to

collimated or diffuse, steady-state monochromatic visible excitation light.

3. ANALYSIS

Let us consider an area of skin exposed to monochromatic excitation light with wavelength λ_x. The excitation source could be a diffuse lamp or a collimated laser. The fluorescent light emitted by the skin is then transported to the detector by means of an optical guide strategically placed. The field of illumination is assumed to be wider than the total skin thickness ($\sim$2 mm) so that the problem can be treated as one-dimensional.

The transport of excitation and fluorescence light in skin is governed by the steady-state radiative transfer equation (RTE) for absorbing, emitting and scattering media. The excitation intensity I_{λ_x} at wavelength λ_x and in direction $\hat{\mathbf{s}}$, satisfies the steady-state RTE expressed as,[32]

$$(\hat{\mathbf{s}} \cdot \nabla) I_{\lambda_x} = -\kappa_{\lambda_x} I_{\lambda_x} - \sigma_{s,\lambda_x} I_{\lambda_x} + \frac{\sigma_{s,\lambda_x}}{4\pi} \int_{4\pi} I_{\lambda_x}(\hat{\mathbf{s}}_i) \Phi_{\lambda_x}(\hat{\mathbf{s}}_i, \hat{\mathbf{s}}) \mathrm{d}\Omega_i \tag{1}$$

where κ_{λ_x} and σ_{s,λ_x} are the linear absorption and scattering coefficients at the excitation wavelength, respectively. The scattering phase function $\Phi_{\lambda_x}(\hat{\mathbf{s}}_i, \hat{\mathbf{s}})$ represents the probability that radiation propagating in direction $\hat{\mathbf{s}}_i$ be scattered into the cone $\mathrm{d}\Omega$ around the direction $\hat{\mathbf{s}}$. The first and second terms on the right hand side represent attenuation of the radiation intensity by absorption and scattering, respectively. The last term corresponds to the augmentation of radiation due to in-scattering. Note that here, the emission by the medium has not been accounted for. Indeed, the radiation

emitted by a blackbody at the normal body temperature of 37°C and at the excitation wavelength is assumed to be negligible compared with the excitation intensity.

Moreover, a similar equation can be written for the transport of fluorescent light emitted by the fluorophores at wavelength λ_F,

$$(\hat{\mathbf{s}} \cdot \nabla) I_{\lambda_F} = -\kappa_{\lambda_F} I_{\lambda_F} - \sigma_{s,\lambda_F} I_{\lambda_F} + \frac{\sigma_{s,\lambda_F}}{4\pi} \int_{4\pi} I_{\lambda_F}(\hat{\mathbf{s}}_i) \Phi_{\lambda_F}(\hat{\mathbf{s}}_i, \hat{\mathbf{s}}) \mathrm{d}\Omega_i + \beta_{\lambda_x} G_{\lambda_x}/4\pi \quad (2)$$

The last term in Equation (2) represents fluorescence emission stimulated by the excitation light coming from all directions. Thus, G_{λ_x} is the fluence defined as $\int_{4\pi} I_{\lambda_x} \mathrm{d}\Omega$. The intrinsic fluorescence coefficient β_{λ_x} is the product of the fluorophore contribution to the overall absorption coefficient at the excitation wavelength λ_{λ_x} denoted by $\kappa_{\lambda_{xF}}$ and the quantum yield QY_{λ_x} of fluorescence emission, i.e, $\beta_{\lambda_x} = \kappa_{\lambda_{xF}} QY_{\lambda_x}$.

The Henyey-Greenstein phase function was used to account for the anisotropic nature of scattering by each layer of the skin and is expressed as,

$$\Phi_\lambda(\Theta) = \frac{1 - g_\lambda^2}{[1 + g_\lambda^2 - 2g_\lambda \cos\Theta]^{3/2}} \quad (3)$$

where, g_λ is the so-called spectral scattering asymmetry factor and Θ is the angle between the directions $\hat{\mathbf{s}}_i$ and $\hat{\mathbf{s}}$.

In order to model fluorescent light transport in skin, one needs (i) a model of the skin morphology, (ii) the optical properties of the skin layers at the excitation and emission wavelengths, and (iii) the spatial distribution of the fluorophores and their fluorescence coefficient β_{λ_x}. The optical model of human skin developed by Zeng *et al.*[27] has been used in the present study to predict the steady-state directional diffuse

reflectance and fluorescence from human skin. This model was chosen among others because (i) it presents a complete and consistent set of properties and (ii) it was validated against experimental data for steady-state autofluorescence of human skin. Thus, the skin is modelled as a seven layered structure whose thicknesses and optical properties at wavelengths 442 and 520 nm are reproduced in Table 2.

Furthermore, two different boundary conditions at the skin surface are considered. The skin sample can be directly exposed to air and thus, there is a mismatch in the refractive index across the skin-air interface. Then, a photon coming from within the tissue and reaching the interface at an angle greater than the critical angle is reflected back into the tissue. The critical angle is defined as $\theta_c = \arcsin(1/n_{sc})$ where n_{sc} is the refractive index of the stratum corneum. The air-skin interface and the interfaces between the skin layers are inherently rough and have to be accounted for in simulations to understand their influence on the distribution of excitation and fluorescence light in skin.[43] However, for the sake of simplicity, the skin-air interface and the interfaces between the skin layers are assumed to be optically smooth in the present simulations. Then, the incident light is reflected and refracted according to Snell's law and the transmitted and reflected intensities computed using Fresnel's equations as commonly performed,[42]

$$\begin{aligned} \rho(\theta_i) &= \frac{1}{2}\left[\frac{sin^2(\theta_i-\theta_t)}{sin^2(\theta_i+\theta_t)}+\frac{tan^2(\theta_i-\theta_t)}{tan^2(\theta_i+\theta_t)}\right] \quad for \quad \theta_i \leq \theta_c, \qquad (4) \\ \rho(\theta_i) &= 1 \quad for \quad \theta_i > \theta_c \end{aligned}$$

where, ρ is the proportion of intensity reflected for a given angle of incidence θ_i, and θ_t, the angle of transmittance given by Snell's law i.e, $\sin\theta_t = n_{sc}\sin\theta_i$. Alternatively, an index matching cream can be applied onto the skin thus, eliminating the total internal reflection at the skin-air interface.

Moreover, in spite of varying refractive indices within the skin, reflection and refraction effects at the interfaces between skin layers are considered negligible as the difference in refractive index between these layers is very minimal (see Table 2). Instead, only the speed of light, $c = c_0/n$, was varied in each layer. Had there been a larger change in the refractive indices between adjacent layers, then the RTE would have had to be solved in each layer separately with the appropriate boundary conditions.

Furthermore, the effects of the directionality of the excitation light on the directional reflectance and fluorescence has also been investigated. This is of practical importance as the incident light can be (i) collimated if the excitation source is a laser or (ii) diffuse if it is a lamp.

Finally, Equations (1) and (2) are solved successively using the modified method of characteristics[3] for (1) collimated or diffuse excitation and (2) with or without an index matching cream applied between the skin and the detector.

The conventional method of characteristics consists of transforming a hyperbolic partial differential equation in to a set of ordinary differential equations which are solved along the characteristic curves. It is based on a Lagrangian formulation, which

identifies photons at an initial time and follows them along the characteristic curves at subsequent times as they are transported. Characteristics are pathlines of photons in the physical space along which information propagates. Though the conventional method yields accurate solutions, it suffers from problems related to grid deformation due to non-uniform velocities of the particles being traced. The modified method of characteristics is a variation of this approach and makes use of a fixed grid and traces particles backward in space from each of the grid points and thus overcomes the problem of grid deformation. In this method of solving the radiative transfer equation (RTE) in three-dimensions, the RTE is converted to an ordinary integro-differential equation and three ordinary differential equations in time, one for each spatial dimension. These equations are then solved at each location and for each direction using standard numerical procedures for ordinary differential equations. Further details about the procedure can be found elsewhere[3] and need not be repeated here.

4. RESULTS AND DISCUSSION

Simulations of directional reflectance and fluorescence of human skin exposed to collimated or diffuse irradiation were performed using a discretization of N_z points along the $z-$direction and N_θ discrete polar angles for θ varying from 0 to π. The numerical results were considered to be converged for $N_z = 226$ and $N_\theta = 181$. For example, a grid size of $N_z = 311$ points along the z-direction and $N_\theta = 181$ polar angles resulted in a change of less than 1% in the computed values of G_{λ_x} for the case of diffuse exci-

tation without an index matching cream. A discretization of $N_z = 226$ and $N_\theta = 241$ resulted in a change of less than 2% in G_{λ_x} for the same configuration. The number of points used for each skin layer is reported in Table 2.

4.A. Collimated Excitation Light

The case of skin exposed to collimated excitation light was considered first. An emissive power or intensity of 10,000 W/m^2 was imposed normally onto the skin. Figure 1 compares the steady-state profile of the excitation fluence $G_{\lambda_x}(z)$ in the skin at $\lambda_x =$ 442 nm obtained in the present study with that obtained by Zeng *et al.*[27] using the Monte Carlo method. Unlike the present study, the computer program used by Zeng *et al.*[27] accounts for mismatches in the refractive index between adjacent skin layers. However, the values of fluence G_{λ_x} predicted by the modified method of characteristics in the case without an index matching cream fall within 5% of that predicted by Zeng *et al.*[27] at all points except in the stratum-corneum where the difference reaches up to 10%. Thus, given the uncertainty in the optical properties of each layer, it can be concluded that the small differences in the refractive indices between adjacent layers can be ignored in numerical simulations.

Moreover, the fluence G_{λ_x} is reduced by 1 to 5 % at the air-skin interface when an index matching cream is applied. Indeed, using an index matching cream eliminates total internal reflection at the surface of the skin. Thus, more light escapes from the skin and decreases the fluence within the skin. Note also that the fluence distribution

is similar in both cases within the deeper layers of the skin and decays rapidly into the skin. In all cases, beyond 600 μm in the reticular dermis, the excitation light intensity becomes negligibly small.

Directional Diffuse Reflectance

The overall reflectance of human skin consists of the specular and diffuse reflectances. The specular reflectance from the skin is computed using Fresnel's laws for the light incident onto the skin. For collimated excitation incident normally, the specular reflectance is given by $\rho(0) = \frac{(n_{sc}-1)^2}{(n_{sc}+1)^2} = 3.4$ % at 442 nm corresponding to an intensity of 337 W/m^2sr in direction $\theta = 0^o$. The diffuse reflectance on the other hand corresponds to the light back-scattered after it has travelled through the skin. Figure 2 shows the angular profile of the steady-state diffuse reflectance of human skin with and without an index matching cream under monochromatic collimated light at $\lambda_x = 442$ nm. The profile of the diffuse reflectance from skin in both cases is relatively isotropic and not as anisotropic as one would expect for a highly forward scattering medium like skin. The diffuse reflectance from skin depends on the separation distance between the source and detector. As the distance between these increases, the depth of skin probed increases. In fact it was shown by Meglinski *et al.*[44] that the diffuse reflectance from skin with the source-detector separation at 250 μm was from tissue within 100 μm from the surface. The present study makes use of a wide beam illumination and reflectance is measured at the center of this beam

and thus the source-detector separation is equivalently zero. As a result, the major contribution to the diffuse reflectance is from photons back-scattered by the topmost layers of the tissue. Thus, the directional profile of the diffusely reflected intensity resembles the quasi-isotropic back-scattering profile for a highly forward scattering medium.

Moreover, a small difference can be seen in the directional profiles of the diffuse reflectance of skin with and without an index matching cream. The reflected intensities obtained by using an index matching cream were higher than those obtained without an index matching cream. This can be attributed to the presence of total internal reflection in the case of a mismatch in refractive index resulting in lower reflected intensities from the skin.

Directional Fluorescence

Several studies have reported numerical results showing the spectral *hemispherical* distribution of fluorescent light from skin.[27,34–36] The present study expands on previous work by reporting the *directional* autofluorescence of skin under steady-state collimated exposure at 442 nm. Figure 3 shows the angular distribution of fluorescent light at 520 nm from human skin excited by collimated light at 442 nm with and without an index matching cream. Unlike steady-state diffuse reflectance, the directional fluorescence intensity is highly anisotropic and concentrated in the direction normal to the skin. This is due to the fact that the fluorescence signal is due to photons

emitted from deeper in the skin and emerging at the skin surface after having been multiply scattered. In addition, the fluorescence intensity with an index matching cream applied onto the skin is lower than without an index matching cream. At any point in the skin, the fluorescence intensity depends on the irradiance G_{λ_x}. The latter is reduced when an index matching cream is used resulting in a lower fluorescence intensity.

The hemispherical fluorescence can be computed by integrating the directional fluorescence over an hemisphere,

$$R_{\lambda_F} = -2\pi \int_{\pi/2}^{\pi} I_{\lambda_F}(0,\theta) cos\theta sin\theta \mathrm{d}\theta \tag{5}$$

where θ is measured from the $z-$axis. The value of R_{λ_F} at 520 nm with and without an index matching cream is $84.5 W/m^2$ and $106.25 W/m^2$. Unfortunately Zeng *et al.*[27] normalized all the values of fluorescence to the maximum value (set to 100) and no quantitative comparisons could be made.

4.B. Diffuse Excitation

Recently, Meerwaldt *et al.*[18] proposed an "autofluorescence reader" to study skin autofluorescence from patients with type 1 and type 2 diabetes. The device made use of a UV lamp for excitation and an optical fiber for collecting the fluorescence signal. Optimal design of such an instrument would require an analysis of directional reflectance and fluorescence from skin after being excited by diffuse light. Therefore, the case of diffuse excitation light such as that produced by a lamp is now considered.

A uniform incident intensity profile of the form $I_{\lambda_x}(z = 0, 0 \leq \theta \leq \pi/2) = 10,000/\pi$ $W/m^2.sr$ is incident onto the skin surface. This value was chosen so that the same emissive power incident on the skin was used for both diffuse and collimated excitation simulations. A part of this incident light is specularly reflected and the remaining transmitted into the skin. The proportions of light reflected and transmitted are computed using Fresnel's laws

Figure 4 compares the steady-state excitation fluence $G_{\lambda_x}(z)$ profile in the skin for diffuse excitation light with and without an index matching cream. There is a large difference of up to 65 % in the value of G_{λ_x} with and without an index matching cream. This is due to the fact that without an index matching cream, light incident on the skin is reflected off the skin surface and only a fraction of this incident light is able to penetrate into the skin.

Furthermore, the fluence G_{λ_x} in the stratum corneum and the top of the epidermis for diffuse excitation with an index matching cream is larger than that for collimated excitation by up to 90%. On the contrary, in the deeper layers of the skin, the fluence obtained using collimated excitation is higher than for diffuse excitation by up to 30%. Indeed, when the excitation light is collimated, the entire energy is concentrated in a single direction into the skin. Since each layer of the skin is a strongly forward scattering medium the excitation light is able to penetrate deep into the skin. On the other hand, in diffuse excitation, only a part of the energy is directed normally onto the skin and so the fluence decreases for locations deeper in the skin. This indicates that

fluorescence emitted from diffuse excitation comes for a large part from fluorophores located in the topmost layer of the skin. On the contrary, collimated excitation tends to sense fluorophores located deeper in the skin.

Directional Diffuse Reflectance

Figure 5 shows the angular profile of the steady-state diffuse and total (diffuse and specular) reflectance of human skin with and without an index matching cream under diffuse excitation light at $\lambda_x = 442$ nm. Unlike collimated incidence, the directional diffuse reflectance is strongly affected by the presence of an index matching cream. The emissive power in diffuse excitation is distributed over the entire hemisphere unlike collimated excitation where the entire energy is concentrated in a single direction. As a result, the values of reflected intensity at angles close to $\pi/2$, due to contributions from photons incident at θ close to $\pi/2$, are much larger for diffuse excitation than for collimated excitation.

In the absence of an index matching cream, only a small fraction of the incident light is able to penetrate the skin due to specular reflection at the skin-air interface. Also, photons incident on the skin-air interface at angles greater than the critical angle within the skin are reflected back into the skin. The combination of these two effects results in a lower intensity of the diffusely reflected excitation light in all directions.

Directional Fluorescence

Figure 6 shows the angular distribution of fluorescent light from human skin exposed to diffuse excitation with and without an index matching cream. The fluorescence intensity from the skin without an index matching cream is lower than that of skin with an index matching cream. This can be attributed to the lower value of G_{λ_x} within the skin observed in the absence of an index matching cream. Moreover, the directional fluorescence intensity profiles are similar to those obtained for collimated excitation. Indeed, the fluorescence depends only on the excitation fluence G_{λ_x}. Thus, the directional profile of the fluorescence is independent of the directional nature of the excitation source. However, because of the larger fluence, the fluorescence intensity is larger for collimated than for diffuse excitation light by about 38.5% with an index matching cream and 61% without an index matching cream at the maximum, i.e. at $\theta = 0^o$.

5. CONCLUSIONS

This paper presented the steady-state directional reflectance at 442 nm and fluorescence at 520 nm from human skin using a novel numerical technique to solve the radiative transfer equation. The skin was treated as a seven layer medium with optically smooth interfaces. Collimated and diffuse excitations at 442 nm were considered with and without an index matching cream to eliminate total internal reflection. The following conclusions can be drawn for collimated excitation light,

- The diffuse reflectance is nearly isotropic with or without an index matching cream. The major contribution to the reflectance is from photons back-scattered from the stratum corneum and thus the reflectance profile resembles the quasi-isotropic back-scattering profile of the Henyey Greenstein phase function for $g = 0.9$.

- The use of an index matching cream increases the diffuse reflectance but decreases the fluorescence from skin. The use of an index matching cream increases the amount of light escaping from the skin, thus increasing the reflectance and decreasing the fluence within the skin. The lower fluence in turn results in a lower fluorescence emission from the skin.

For diffuse excitation light,

- The diffuse reflectance is nearly isotropic when skin is directly exposed to air, while the presence of an index matching cream increases the refleceted intensity at angles close to $\theta = \pi/2$ and distorts the isotropic profile.

- The use of an index matching cream increases *both* the diffuse reflectance and autofluorescence of skin. The use of an index matching cream allows a greater amount of light to penetrate the skin. This then, results in an increased reflectance and fluorescence from the skin.

- In both cases, the fluorescence is anisotropic and focused along the normal to the skin.

These results are of particular importance with the rising interest in studying the effect of cosmetics on skin, pharmacokinetics, and non-invasive diagnosis of various diseases which alter the autofluorescence and diffuse reflectance properties of human skin. Predicting the directional reflectance and fluorescence profiles can also be very valuable in designing probes and other optics for biomedical applications.

References

1. J. R. Lakowicz, *Principles of Fluorescence Spectroscopy* (Kluwer Academic/Plenum Publishers, New York, NY, 1999).
2. R. Richards-Kortum and E. Sevick-Muraca, "Quantitative optical spectroscopy for tissue diagnostics," Annual Review of Physical Chemistry **47**, 555–606 (1996).
3. K. Katika and L. Pilon, "Modified method of characteristics in transient radiative transfer," Journal of Quantitative Spectroscopic and Radiative Transfer **(in press)** (2005).
4. H.Zeng and C. MacAulay, "Fluorescence Spectroscopy and Imaging for skin cancer detection and evaluation," in *Handbook of Biomedical Fluorescence*, pp. 315–360 (Marcel Dekker, 2003).
5. M. J. C. V. Gemert, S. L. Jacques, H. J. C. M. Sterenborg, and W. M. Star, "Skin Optics," IEEE Transactions on Biomedical Engineering **36**(12), 1146–1154 (1989).
6. N. Kollias, G. Zonios, and G. N. Stamatas, "Fluorescence spectroscopy of skin,"

Vibrational Spectroscopy **28**, 17–23 (2002).

7. K. Koenig, H. Schneckenburger, J. Hemmer, B. J. Tromberg, and R. W. Steiner, "In-vivo fluorescence detection and imaging of porphyrin-producing bacteria in the human skin and in the oral cavity for diagnosis of acne vulgaris, caries, and squamous cell carcinoma," in *Advances in Laser and Light Spectroscopy to Diagnose Cancer and Other Diseases*, R. R. Alfano, ed., vol. 2135, pp. 129–138 (SPIE, 1994).

8. Y. Takema, Y. Yorimoto, H. Ohsu, O. Osanai, and M. Kawai, "Age-related discontinuous changes in the in vivo fluorescence of human facial skin," Journal of Dermatological Science **24**, 55–58 (1997).

9. N. Kollias, R. Gillies, M. Moran, I. E. Kochevar, and R. R. Anderson, "Endogenous Skin Fluorescence Includes Bands that may Serve as Quantitative Markers of Aging and Photoaging," Journal of Investigative Dermatology **111**(5), 776–776 (1998).

10. R. H. Na, I. M. Stender, M. Henriksen, and H. C. Wulf, "Autofluorescence of human skin is age-related after correction for skin pigmentation and redness," Journal of Investigative Dermatology **116**, 536–540 (2001).

11. J. Sandby-Moller, E. Thieden, P. A. Philipsen, J. Heydenreich, and H. C. Wulf, "Skin autofluorescence as a biological UVR dosimeter," Photodermatology Photoimmunology and Photomedicine **20**(1), 33–40 (2004).

12. R. Gillies, G. Zonios, R. R. Anderson, and N. Kollias, "Fluorescence excitation spectroscopy provides information about human skin in vivo," Journal of Investigative Dermatology **115**(4), 704–707 (2000).

13. L. Brancaleon, A. J. Durkin, J. H. Tu, G. Menaker, J. D. Fallon, and N. Kollias, "In vivo fluorescence spectroscopy of nonmelanoma skin cancer," Photochemistry and Photobiology **73**(2), 178–183 (2001).

14. H. Zeng, D. I. McLean, C. E. MacAulay, B. Palcic, and H. Lui, "Autofluorescence of basal cell carcinoma," in *Lasers in Surgery: Advanced Characterization, Therapeutics, and Systems VIII*, R. R. Anderson, K. E. Bartels, L. S. Bass, C. G. Garrett, K. W. Gregory, H. Lui, R. S. Malek, A. P. Perlmutter, L. Reinisch, P. J. Smalley, L. P. Tate, S. L. Thomsen, and G. M. Watson, eds., vol. 3245, pp. 314–317 (SPIE, 1998).

15. H. Zeng, D. I. McLean, C. E. MacAulay, and H. Lui, "Autofluorescence properties of skin and applications in dermatology," in *Biomedical Photonics and Optoelectronic Imaging*, H. Liu and Q. Luo, eds., vol. 4224, pp. 366–373 (SPIE, 2000).

16. M. Panjehpour, C. E. Julius, M. N. Phan, T. Vo-Dinh, and B. F. Overholt, "In-vivo fluorescence spectropscopy for diagnosis of skin cancer," in *Biomedical Diagnostic, Guidance, and Surgical-Assist Systems IV*, T. Vo-Dinh, D. A. Benaron, and W. S. Grundfest, eds., vol. 4615, pp. 20–31 (SPIE, 2002).

17. T. Vo-Dinh, M. Panjehpour, B. F. Overholt, C. E. Julius, S. Overholt, and M. N.

Phan, "Laser-induced fluorescence for the detection of esophageal and skin cancer," in *Advanced Biomedical and Clinical Diagnostic Systems*, T. Vo-Dinh, W. S. Grundfest, D. A. Benaron, and G. E. Cohn, eds., vol. 4958, pp. 67–70 (SPIE, 2003).

18. R. Meerwaldt, R. Graaff, P. H. N. Oomen, T. P. Links, J. J. Jager, N. L. Alderson, S. R. Thorpe, J. W. Baynes, R. O. B. Gans, and A. J. Smit, "Simple non-invasive assessment of advanced glycation endproduct accumulation," Diabetologia **47**, 1324–1330 (2004).

19. Y. P. Sinichkin, S. R. Utz, and H. A. Pilipenko, "Laser-induced fluorescence of the human skin in vivo: influence of the erythema," in *Optical Biopsy*, R. Cubeddu, S. Svanberg, and H. van den Bergh, eds., vol. 2081, pp. 41–47 (SPIE, 1994).

20. Y. P. Sinichkin, S. R. Utz, P. M. Yudin, and H. A. Pilipenko, "Investigation of formation and dynamics of human skin erythema and pigmentation by in vivo fluorescence spectroscopy," in *Optical Biopsy and Fluorescence Spectroscopy and Imaging*, R. Cubeddu, R. Marchesini, S. R. Mordon, K. Svanberg, H. H. Rinneberg, and G. A. Wagnieres, eds., vol. 2324, pp. 259–268 (SPIE, 1995).

21. S. R. Utz, Y. P. Sinichkin, I. V. Meglinski, and H. A. Pilipenko, "Fluorescence spectroscopy in combination with reflectance measurements in human skin examination: what for and how," in *Optical Biopsy and Fluorescence Spectroscopy and Imaging*, R. Cubeddu, R. Marchesini, S. R. Mordon, K. Svanberg, H. H.

Rinneberg, and G. A. Wagnieres, eds., vol. 2324, pp. 125–136 (SPIE, 1995).

22. H. Zeng, C. E. MacAulay, B. Palcic, and D. I. McLean, "Laser-induced changes in autofluorescence of in-vivo skin," in *Laser-Tissue Interaction IV*, S. L. Jacques and A. Katzir, eds., vol. 1882, pp. 278–290 (SPIE, 1993).

23. H. Zeng, C. E. MacAulay, B. Palcic, and D. I. McLean, "Monte Carlo modeling of tissue autofluorescence measurement and imaging," in *Advances in Laser and Light Spectroscopy to Diagnose Cancer and Other Diseases*, R. R. Alfano, ed., vol. 2135, pp. 94–104 (SPIE, 1994).

24. H. Zeng, C. MacAulay, D. I. McLean, and B. Palcic, "Spectroscopic and Microscopic Characteristics of Human Skin Autofluorescence Emission," Photochemistry and Photobiology **61**, 639–645 (1995).

25. H. Zeng, C. E. MacAulay, D. I. McLean, and B. Palcic, "Spectroscopy and microscopy studies of skin tissue autofluorescence emission," in *Optical Biopsy and Fluorescence Spectroscopy and Imaging*, R. Cubeddu, R. Marchesini, S. R. Mordon, K. Svanberg, H. H. Rinneberg, and G. A. Wagnieres, eds., vol. 2324, pp. 198–207 (SPIE, 1995).

26. H. Zeng, H. Lui, D. I. McLean, C. E. MacAulay, and B. Palcic, "Optical spectroscopy studies of diseased skin: preliminary results," in *Optical and Imaging Techniques for Biomonitoring*, H.-J. Foth, R. Marchesini, H. Podbielska, M. Robert-Nicoud, and H. Schneckenburger, eds., vol. 2628, pp. 281–285 (SPIE,

1996).

27. H. Zeng, C. MacAulay, D. I. McLean, and B. Palcic, "Reconstruction of in vivo skin autofluorescence spectrum from microscopic properties by Monte Carlo simulation," Journal of Photochemistry and Photobiology B: Biology **38**, 234–240 (1997).

28. H. Zeng, C. E. MacAulay, B. Palcic, and D. I. McLean, "Autofluorescence distribution in skin tissue revealed by microspectrophotometer measurements," in *Lasers in Otolaryngology, Dermatology, and Tissue Welding*, R. R. Anderson, L. S. Bass, S. M. Shapshay, J. V. White, and R. A. White, eds., vol. 1876, pp. 129–135 (SPIE, 1993).

29. M. Keijzer, R. Richards-Kortum, S. Jacques, and M. Feld, "Fluorescence spectroscopy of turbid media: Autofluorescence of the human aorta," Applied Optics **28**, 4286–4292 (1989).

30. I. V. Meglinski and D. Y. Churmakov, "A novel Monte Carlo method for the optical diagnostics of skin," in *Diagnostic Optical Spectroscopy in Biomedicine II*, G. A. Wagnieres, ed., vol. 5141, pp. 133–141 (SPIE, 2003).

31. I. V. Meglinski, "Monte Carlo Method in optical diagnostics of skin and skin tissues," in *Third International Conference on Photonics and Imaging in Biology and Medicine*, Q. Luo, V. V. Tuchin, M. Gu, and L. V. Wang, eds., vol. 5254, pp. 30–43 (SPIE, 2003).

32. M. F. Modest, *Radiative Heat Transfer* (Academic Press, San Diego, CA, 2002).

33. D. Y. Churmakov, I. V. Meglinski, S. A. Piletsky, and D. A. Greenhalgh, "Skin fluorescence model based on the Monte Carlo technique," in *Saratov Fall Meeting 2002: Optical Technologies in Biophysics and Medicine IV*, V. V. Tuchin, ed., vol. 5068, pp. 326–333 (SPIE, 2003).

34. D. Y. Churmakov, I. V. Meglinski, and D. A. Greenhalgh, "Amending of fluorescence sensor signal localization in human skin by matching of the refractive index," Journal of Biomedical Optics **9**, 339–346 (2004).

35. D. Y. Churmakov, I. V. Meglinski, and D. A. Greenhalgh, "Automatic amending of the tattoo sensor fluorescence localization by refractive index matching," in *Diagnostic Optical Spectroscopy in Biomedicine II*, G. A. Wagnieres, ed., vol. 5141, pp. 122–132 (SPIE, 2003).

36. D. Y. Churmakov, I. V. Meglinski, S. A. Piletsky, and D. A. Greenhalgh, "Automatic enhancement of skin fluorescence localization due to refractive index matching," in *ALT'03 International Conference on Advanced Laser Technologies: Biomedical Optics*, R. K. Wang, J. C. Hebden, A. V. Priezzhev, and V. V. Tuchin, eds., vol. 5486, pp. 16–27 (SPIE, 2004).

37. A. Ishimaru, "Diffusion of light in turbid material," Applied Optics **28**(12), 2210–2215 (1989).

38. T. J. Farrell and M. S. Patterson, "Diffusion Modeling of Fluorescence in tissue,"

in *Handbook of Biomedical Fluorescence*, pp. 29–60 (Marcel Dekker, 2003).

39. A. H. Hielscher, R. E. Alcouffe, and R. L. Barbour, "Comparison of finite-difference transport and diffusion calculations for photon migration in homogeneous and heterogeneous tissues," Physics in Medicine and Biology **43**, 1285–1302 (1998).

40. T. Spott and L. O. Svaasand, "Collimated light sources in the diffusion approximation," Applied Optics **39**, 6453–6465 (2000).

41. G. Yoon, S. A. Prahl, and A. J. Welch, "Accuracies of the diffusion approximation and its similarity relations for laser irradiated biological media," Applied Optics **28**, 2250–2255 (1989).

42. L.-H. Wang and S. L. Jacques, "Monte Carlo Modeling of Light Transport in Multi-layered Tissues in Standard C," University of Texas M. D. Anderson Cancer Center (1992).

43. J. Q. Lu, X.-H. Hu, and K. Dong, "Modeling of the rough-interface effect on a converging light beam propagating in a skin tissue phantom," Applied Optics **39**, 5890–5897 (2000).

44. I. V. Meglinski and S. J. Matcher, "Modeling of skin reflectance spectra," in *Saratov Fall Meeting 2000: Optical Technologies in Biophysics and Medicine II*, V. V. Tuchin, ed., vol. 4241, pp. 78–87 (SPIE, 2001).

Figure and Table Captions

Figure 1. Excitation light fluence as a function of depth inside skin for $\lambda_x = 442$ nm for collimated excitation light with and without index matching cream.

Figure 2. Steady-state directional diffuse reflectance of skin at $\lambda_x = 442$ nm for collimated excitation light with and without index matching cream.

Figure 3. Steady-state directional fluorescence of skin at $\lambda_F = 520$ nm for collimated excitation light with and without index matching cream.

Figure 4. Excitation light fluence distribution as a function of depth inside skin for $\lambda_x = 442$ nm for diffuse excitation light with and without index matching cream.

Figure 5. Steady-state directional reflectance of skin at $\lambda_x = 442$ nm for diffuse excitation light with and without index matching cream.

Figure 6. Steady-state directional fluorescence of skin at $\lambda_F = 520$ nm for diffuse excitation light with and without index matching cream.

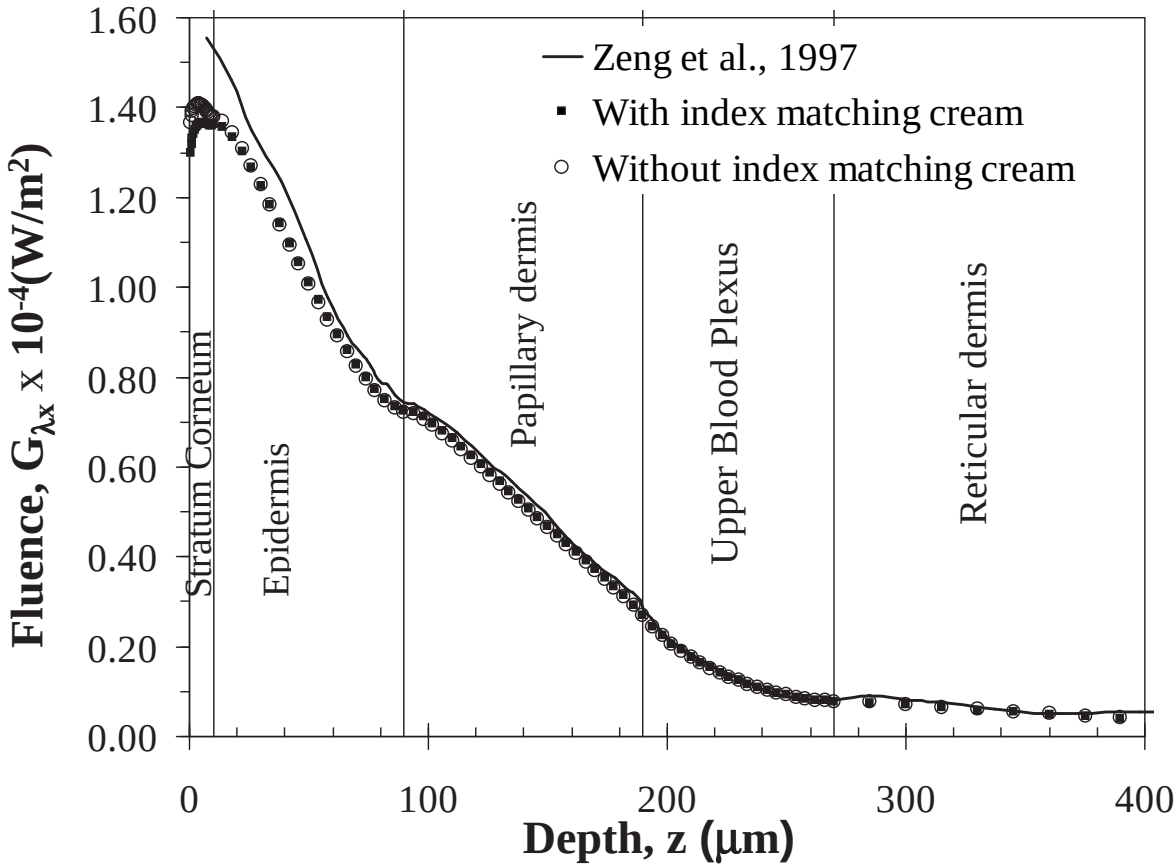

Fig. 1. Excitation light fluence as a function of depth inside skin for $\lambda_x = 442$ nm for collimated excitation light with and without index matching cream.

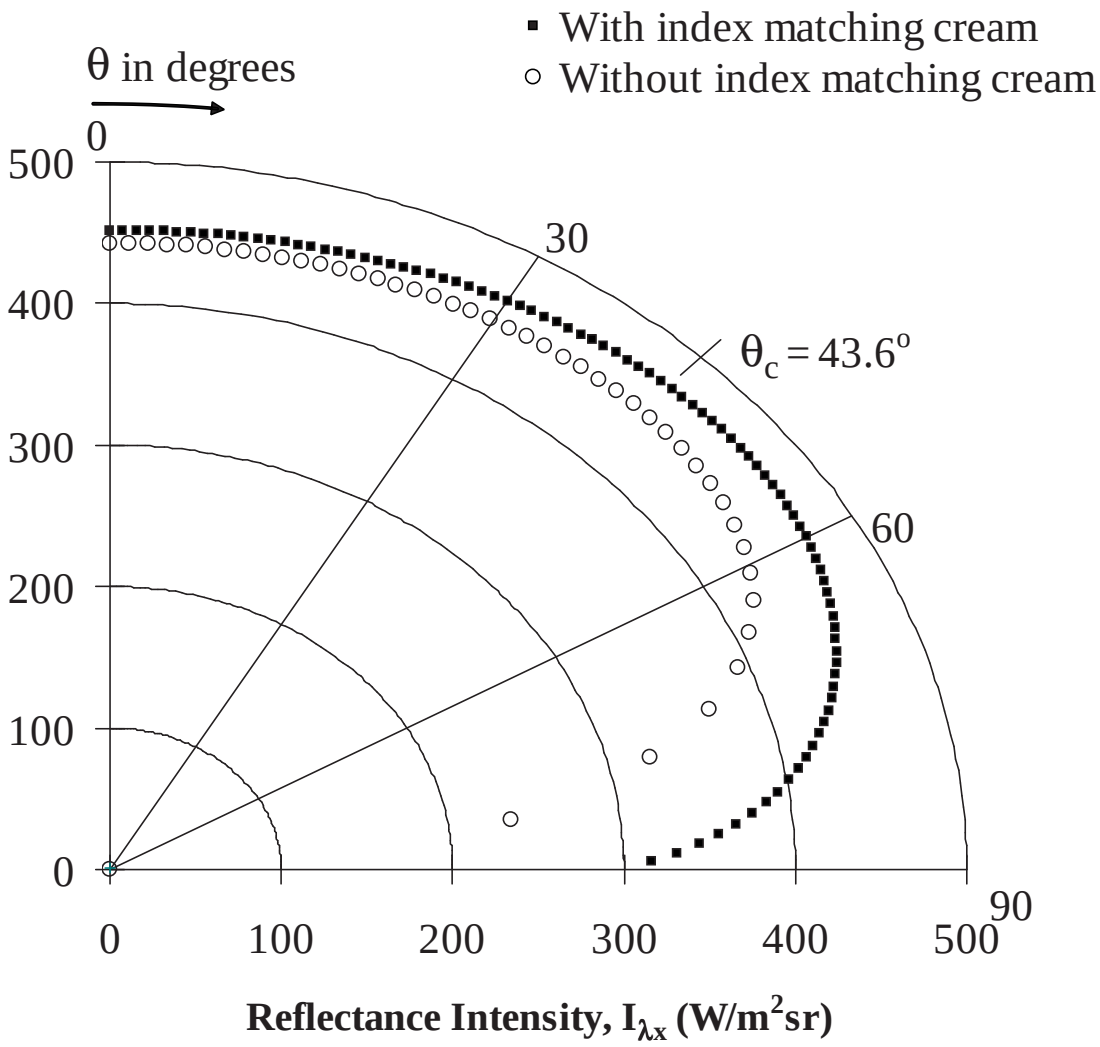

Fig. 2. Steady-state directional diffuse reflectance of skin at $\lambda_x = 442$ nm for collimated excitation light with and without index matching cream.

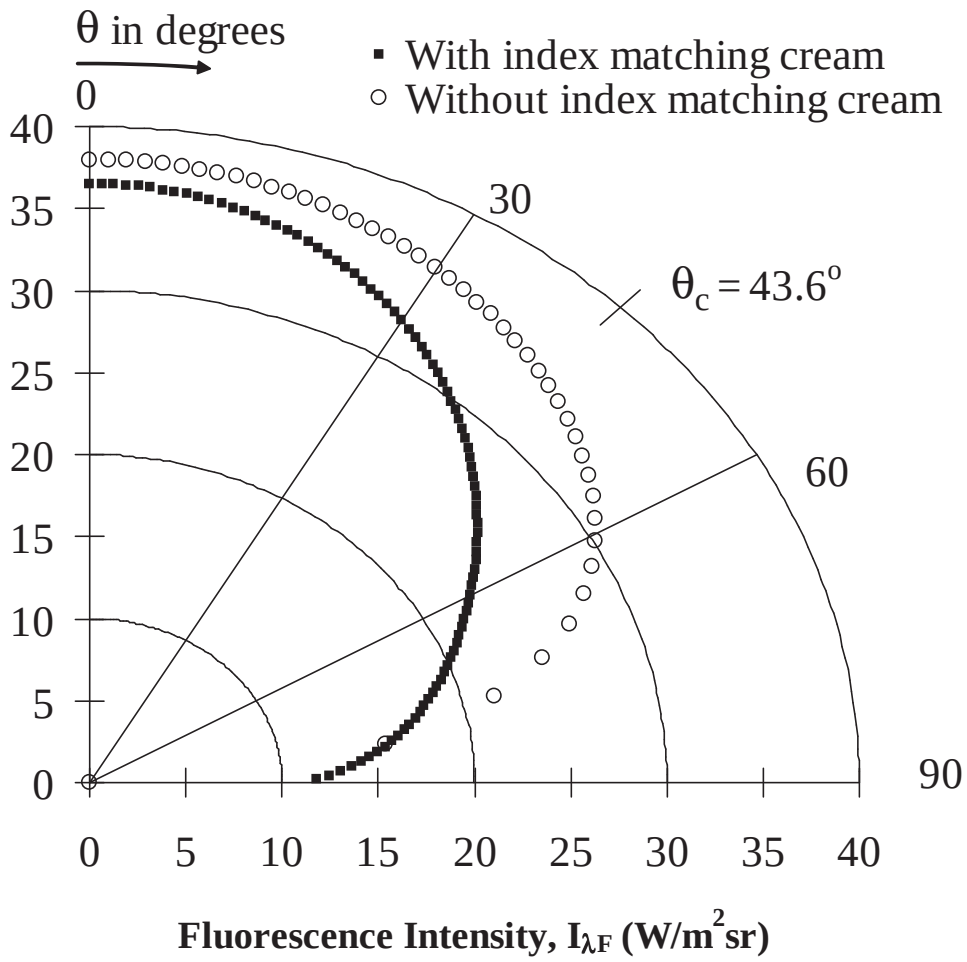

Fig. 3. Steady-state directional fluorescence of skin at $\lambda_F = 520$ nm for collimated excitation light with and without index matching cream.

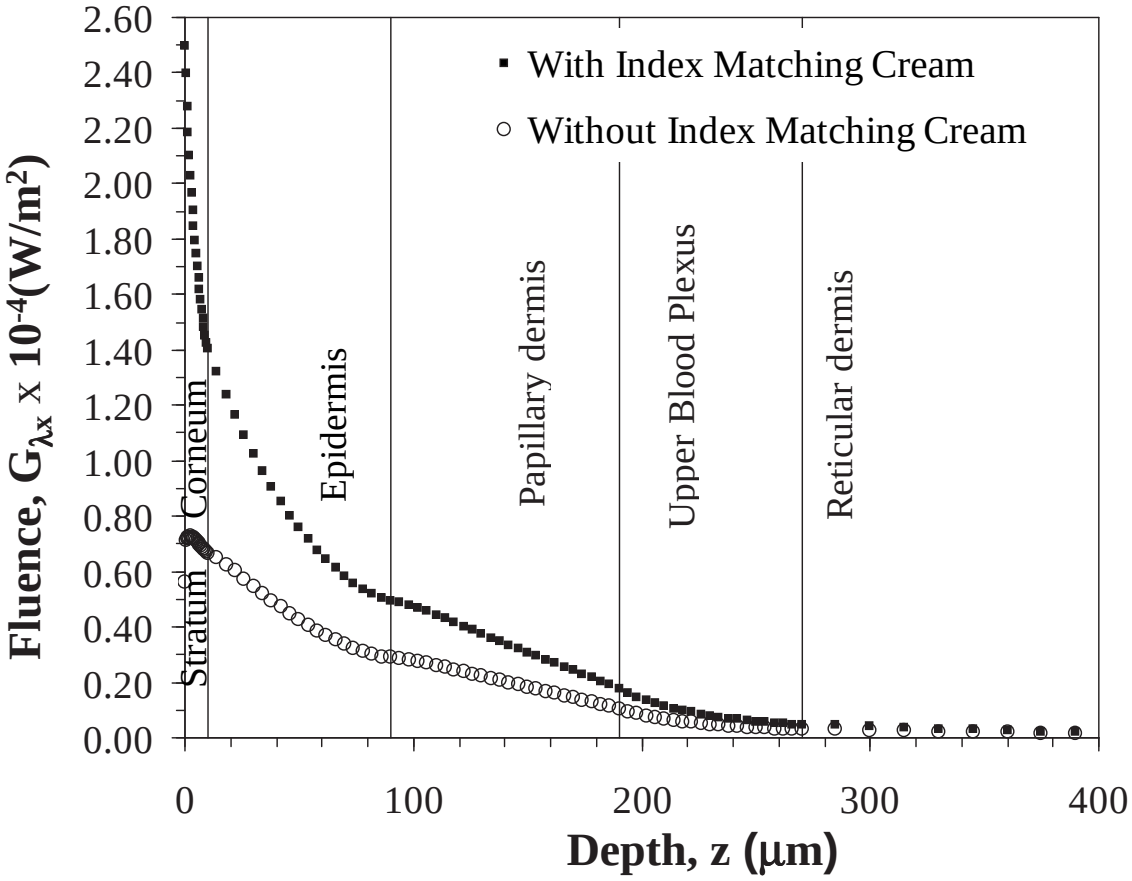

Fig. 4. Excitation light fluence distribution as a function of depth inside skin for $\lambda_x = 442$ nm for diffuse excitation light with and without index matching cream.

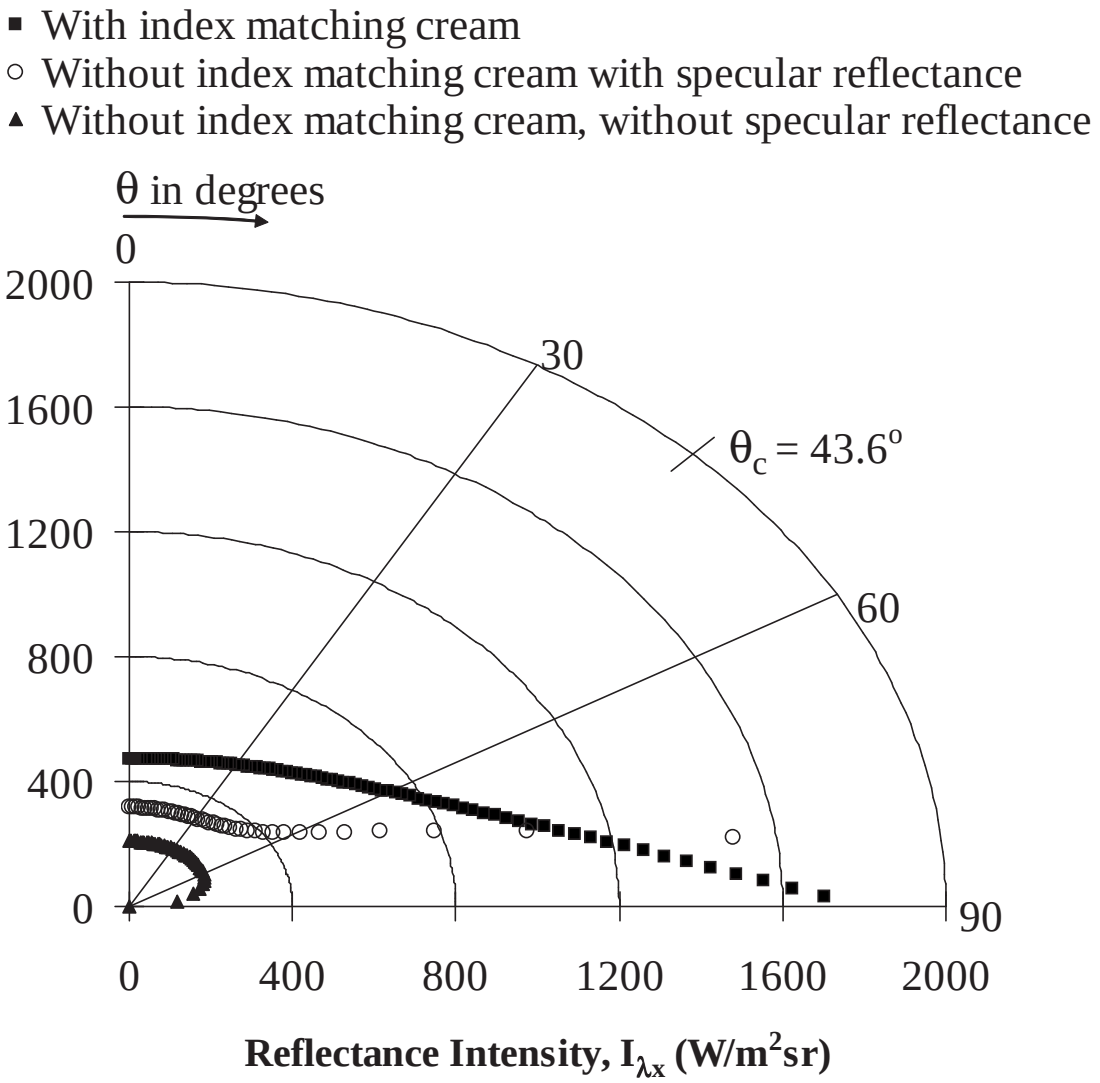

Fig. 5. Steady-state directional reflectance of skin at $\lambda_x = 442$ nm for diffuse excitation light with and without index matching cream.

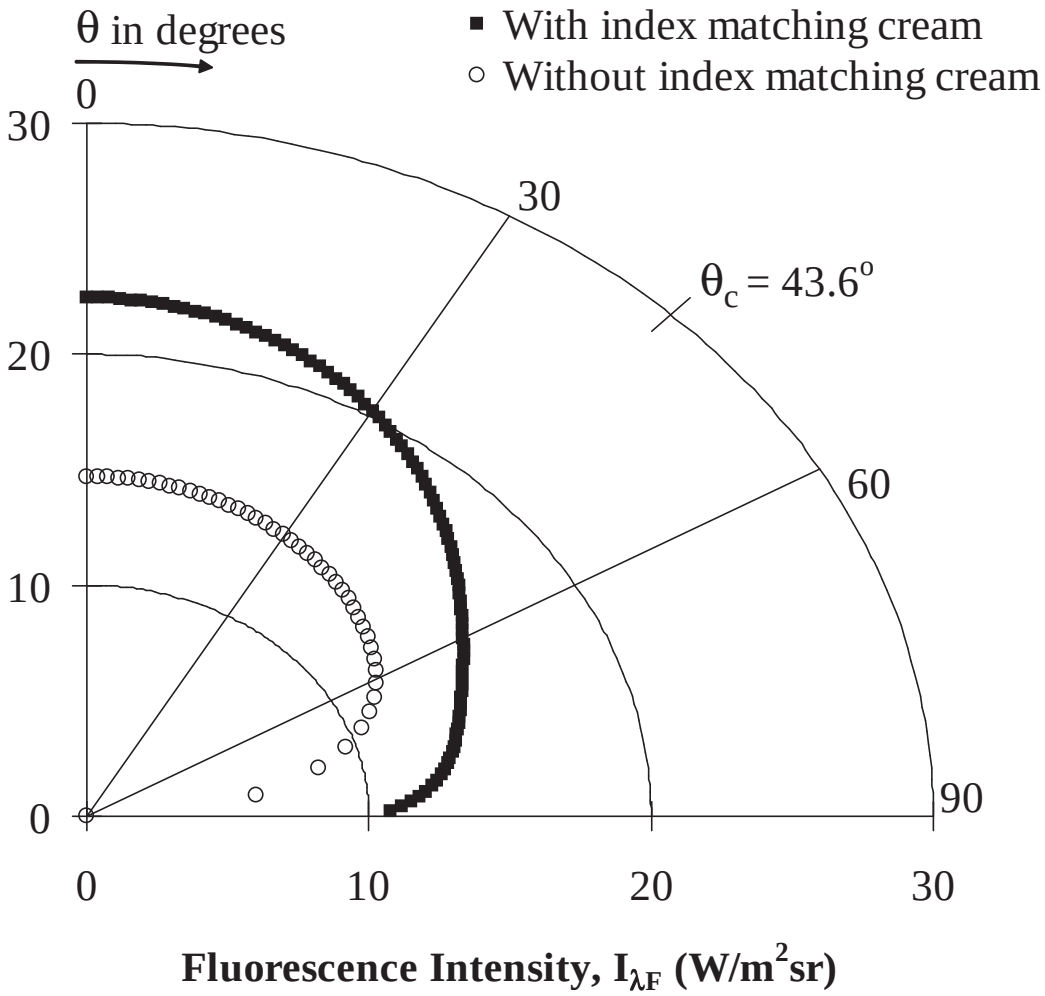

Fig. 6. Steady-state directional fluorescence of skin at $\lambda_F = 520$ nm for diffuse excitation light with and without index matching cream.

Table 1. Summary of experimental studies of steady-state in-vivo fluorescence spectroscopy of human skin.

Ref.	λ_x	λ_F	Application
[7]	407 nm	590-720 nm	acne
[8]	325 nm	390 and 430 nm	aging
[9]	260-460 nm	340-480 nm	aging
[10]	330 nm, 370 nm	375 and 455 nm	aging
[11]	330, 330 and 370 nm	370,455 and 455 nm	aging
[12]	260-480 nm	340-480 nm	psoriasis
[13]	250-400 nm	300-600 nm	skin cancer
[4, 14, 15]	350-470 nm	450-750 nm	skin cancer
[16, 17]	410 nm	430-716 nm	skin cancer
[18]	300-420 nm with a peak at 350 nm	300-600 nm	type 1 and 2 diabetes
[19–21]	337 nm	380-560nm	erythema, pigmentation
[22]	442 nm	490-600 nm	photobleaching
[24, 25]	350-470 nm	400-700 nm	N/A
[26]	442 nm	400-750 nm	N/A

Table 2. Optical properties used in the seven-layer skin model at 442 and 520 nm.[27]

Layer	*Thickness*	n		κ_λ (cm^{-1})		$\sigma_{s,\lambda}$ (cm^{-1})		g_λ		β_λ (cm^{-1})	N_z
	μm	$442nm$	$520nm$	$442nm$	$520nm$	$442nm$	$520nm$	$442nm$	$520nm$	$520nm$	
Stratum Corneum	10	1.45	1.45	190	40	2300	570	0.9	0.77	1.0	20
Epidermis	80	1.4	1.4	56	40	570	570	0.75	0.77	0.0	20
Papillary Dermis	100	1.4	1.4	6.7	5	700	500	0.75	0.77	7.5	25
Upper blood plexus	80	1.39	1.39	67	24.5	680	500	0.77	0.79	7.5	20
Reticular dermis	1500	1.4	1.4	6.7	5	700	500	0.75	0.77	7.5	100
Deep blood plexus	70	1.34	1.34	541	181	520	500	0.96	0.96	7.5	20
Dermis	160	1.4	1.4	6.7	5	700	500	0.75	0.77	7.5	20
Subcutaneous fat	–	1.46	1.46	–	–	–	–	–	–	-	-